

# Generalized optical interferometry for modal analysis in arbitrary degrees of freedom

Ayman F. Abouraddy,<sup>1,\*</sup> Timothy M. Yarnall,<sup>2,3</sup> and Bahaa E. A. Saleh<sup>1</sup>

<sup>1</sup>CREOL, The College of Optics & Photonics, University of Central Florida, Orlando, Florida 32816, USA

<sup>2</sup>19 Chestnut Circle, Merrimack, New Hampshire 03054, USA

<sup>3</sup>Currently with Massachusetts Institute of Technology, Lincoln Laboratory, Lexington, Massachusetts 02420, USA

\*Corresponding author: raddy@creol.ucf.edu

Received March 23, 2012; accepted May 8, 2012;

posted May 10, 2012 (Doc. ID 165317); published July 11, 2012

We generalize the traditional concept of temporal optical interferometry to any degree of freedom of a coherent optical field. By identifying the structure of a unitary optical transformation that we designate the generalized phase operator, we enable optical interferometry to be carried out in any modal basis describing a degree of freedom. The structure of the generalized phase operator is that of a fractional optical transform, thus establishing the connection between fractional transforms, optical interferometry, and modal analysis. © 2012 Optical Society of America  
OCIS codes: 260.3160, 120.3180, 030.4070, 050.4865.

Optical interferometry has been crucial in increasing our understanding of the nature of light and is a technique of fundamental importance in optical metrology and astronomy [1]. In temporal interferometry, for example, a pulse enters a Mach–Zehnder interferometer (MZI) and a delay is swept in one arm, thereby producing an interferogram whose Fourier transform (FT) reveals the power spectrum. In this Letter, we generalize the basic concept of temporal interferometry to other degrees of freedom (DoFs). A central feature of this approach is the identification of an optical transformation that generalizes temporal delay to an arbitrary DoF. For DoFs having a discrete modal basis, we find that the generalized “delay” is a *fractional transform* [2] that has this particular modal basis as eigenfunctions. This result establishes a general methodology for optical interferometry using any DoF, and hence modal analysis in any basis. Furthermore, we extend this scheme to multidimensional interferometry using independent DoFs simultaneously.

Our approach is shown schematically in Fig. 1(a) where the delay in a balanced MZI is replaced with an optical transformation  $\Lambda(\alpha)$ , parameterized by a continuous real scalar  $\alpha$ , that we designate the *generalized phase operator* (GPO). At the MZI output, the optical signal is integrated over all DoFs,  $\alpha$  is swept, and an interferogram  $P(\alpha)$  is recorded. In the usual scenario,  $\alpha$  is a delay  $\tau$  and  $P(\tau)$  is the pulse autocorrelation. Using a GPO in lieu of the delay, this interferometer may be used for modal decomposition of a beam in an arbitrary basis.

We express the field as the superposition of an orthonormal set of modes  $\{\psi_n(x)\}_n$ ,  $E(x) = \sum_n c_n \psi_n(x)$ ,  $c_n = \int dx \psi_n^*(x) E(x)$ , where  $x$  is any DoF of the field. The set  $\{\psi_n(x)\}_n$  need not be countable, whereupon the summation over  $n$  is replaced with integration over a real number  $\xi$ ,  $E(x) = \int d\xi c(\xi) \psi(x, \xi)$ , e.g., the FT of a pulse  $E(t) = \frac{1}{2\pi} \int d\omega c(\omega) e^{-i\omega t}$ . We seek a transformation  $\Lambda$  that introduces a phase term  $e^{i\alpha n}$  between the modes indexed by  $n$ , thus generalizing the effect of a delay  $\tau$ .  $\Lambda$  thus takes the form

$$\Lambda(x, x'; \alpha) = \sum_n e^{i\alpha n} \psi_n(x) \psi_n^*(x'). \quad (1)$$

After traversing  $\Lambda$ , the field is  $E_o(x; \alpha) = \int dx' \Lambda(x, x'; \alpha) E(x') = \sum_n e^{i\alpha n} c_n \psi_n(x)$ , and the resulting interferogram  $P(\alpha)$  is

$$P(\alpha) = 1 + \Re \int dx E(x) E_o^*(x; \alpha) = 1 + \sum_n |c_n|^2 \cos \alpha n. \quad (2)$$

Spectral analysis of  $P(\alpha)$  thus reveals the modal weights  $|c_n|^2$ . Note that  $\Lambda$  is unitary,  $\int dx \Lambda(x, x'; \alpha) \Lambda^*(x, x''; \alpha) = \delta(x' - x'')$ ,  $\forall \alpha$ , and the set of transformations  $\{\Lambda(\alpha)\}$  has the structure of a one-parameter (commutative) group under the composition rule  $\Lambda(\alpha_2) \circ \Lambda(\alpha_1) = \Lambda(\alpha_1 + \alpha_2)$  since  $\int dx' \Lambda(x, x'; \alpha_2) \Lambda(x', x''; \alpha_1) = \Lambda(x, x''; \alpha_1 + \alpha_2)$ . The identity is  $\Lambda(x, x'; 0) = \delta(x - x')$ , and the inverse of  $\Lambda(x, x'; \alpha)$  is  $\Lambda^{-1}(x, x'; \alpha) = \Lambda(x, x'; -\alpha)$ . The definition of  $\Lambda$  in Eq. 1 implies that the group is cyclic with period  $2\pi$ :  $\Lambda(\alpha + 2m\pi) = \Lambda(\alpha)$ ,  $\forall m$  integer.

In addition to the group structure of the set  $\{\Lambda\}$ , it is endowed with the structure of a *fractional transform* [2] when the modal set is discrete. Therefore, a fractional transform having the form of Eq. (1) is a GPO operating on its eigenfunction basis. We proceed to show that GPOs corresponding to modal sets of importance in optics may be readily realized (see Table 1). For *time-harmonics*  $\{e^{-i\omega t}\}_\omega$ ,  $\Lambda_1(t, t'; \tau) = \frac{1}{2\pi} \int d\omega e^{-i\omega(t-t'-\tau)} = \delta(t-t'-\tau)$ ;  $\Lambda_1$  is a delay, as expected. For *spatial harmonics*  $\{e^{ikx}\}_k$ ,  $\Lambda_2(x, x'; \Delta) = \delta(x - x' + \Delta)$  is a transverse shift  $\Delta$  [3], while for *polarization*,  $\Lambda_3(\theta)$  is a wave plate introducing a phase  $\theta$  between horizontal  $H$  and vertical  $V$  polarization modes. In the *orbital angular momentum* (OAM) basis  $\{e^{i\ell\phi}\}_\ell$  [4],  $\Lambda_4(\phi, \phi'; \theta) = \delta(\phi - \phi' + \theta)$  is a rotation  $\theta$  [5] (see also Refs. [6,7]). In the *radial Laguerre–Gaussian*

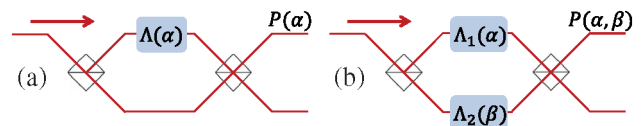
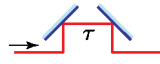
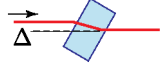
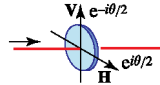
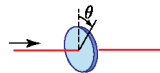
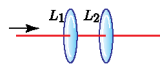
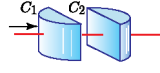



Fig. 1. (Color online) Generalized interferometry using a balanced MZI with (a) a transformation  $\Lambda$  in one arm for analyzing one DoF, or (b)  $\Lambda_1$  and  $\Lambda_2$  for analyzing two DoFs.

**Table 1. Realizations of GPOs for Generalized Interferometry**

Degree of Freedom	Modes	GPO	Realization	Implementation
Temporal spectrum	$\{e^{-i\omega t}\}_\omega$	$\Lambda_1(t, t'; \tau) = \delta(t - t' - \tau)$	Delay $\tau$	
Spatial spectrum	$\{e^{ikx}\}_k$	$\Lambda_2(x, x'; \Delta) = \delta(x - x' + \Delta)$	Transverse shift $\Delta$	
Polarization	$\{H, V\}$	$\Lambda_3(\theta) = \begin{bmatrix} e^{i\theta/2} & 0 \\ 0 & e^{-i\theta/2} \end{bmatrix}$	Retardation $\theta$	
Angular momentum	$\{e^{i\ell\varphi}\}_\ell$	$\Lambda_4(\varphi, \varphi'; \theta) = \delta(\varphi - \varphi' + \theta)$	Rotation $\theta$	
Radial modes	$\{L_p^{ \ell }(r)\}$	$\Lambda_5(r, r'; \alpha) = K_p(r, r'; \alpha)$	fHT of order $\alpha$	
Transverse modes	$\{H_n(x)\}_n$	$\Lambda_6(x, x'; \alpha) = F(x, x'; \alpha)$	fFT of order $\alpha$	
Spatial parity	$\{e, o\}$	$\Lambda_7(x, x') = \delta(x + x')$	Spatial flip	

(LG) basis  $\{L_p^{|\ell|}(r)\}_p$ , one may show that  $\Lambda_5(r, r'; \alpha, |\ell|) = \sum_p e^{ip\alpha} L_p^{|\ell|}(r) L_p^{|\ell|}(r')$  is the fractional Hankel transform (fHT) [8–10] (implemented using two spherical lenses  $L_1$  and  $L_2$  in Table 1). In the 1D Hermite–Gaussian (HG) basis  $\{H_n(x)\}_n$ ,  $\Lambda_6(x, x'; \alpha) = \sum_n e^{in\alpha} H_n(x) H_n^*(x')$  is the fractional Fourier transform (fFT) of order  $\frac{2\alpha}{\pi}$  [2, 11] (implemented using two cylindrical lenses  $C_1$  and  $C_2$  in Table 1). Setting  $\theta = \pi$ ,  $\Lambda_7(x, x') = \Lambda_6(x, x'; \pi) = \delta(x + x')$  enables the field to be analyzed into its even ( $e$ ) and odd ( $o$ ) components (i.e., its spatial parity). This GPO is realized by spatial flip along  $x$  [12–15] implemented by a mirror or a Dove prism. We have therefore established that the construction of GPOs is feasible for typical optical DoFs and potentially for arbitrary DoFs.

Next we consider a field described by two DoFs,  $x$  and  $y$ , expressed in terms of two modal sets,  $E(x, y) = \sum_{nm} c_{nm} \psi_n(x) \phi_m(y)$ . In order to perform 2D optical interferometry, and hence analyze the field into the sets  $\{\psi_n(x)\}_n$  and  $\{\phi_m(y)\}_m$ , we place the GPOs corresponding to each,  $\Lambda_1(x, x'; \alpha)$  and  $\Lambda_2(y, y'; \beta)$ , respectively, in a balanced MZI [Fig. 1(b)]. The 2D interferogram  $P(\alpha, \beta)$  is

$$\begin{aligned} P(\alpha, \beta) &= 1 + \Re \iint dx dy E_1(x, y; \alpha) E_2^*(x, y; \beta) \\ &= 1 + \sum_{nm} |c_{nm}|^2 \cos(n\alpha - m\beta); \end{aligned} \quad (3)$$

here  $E_1$  and  $E_2$  are the fields after traversing  $\Lambda_1$  and  $\Lambda_2$ , respectively. Performing a 2D FT on  $P(\alpha, \beta)$  thus reveals the 2D modal weights  $|c_{nm}|^2$ .

As an example, consider a field resulting from the superposition of an OAM mode  $E_1(r, \varphi) = e^{i\ell\varphi} L_p^{|\ell|}(r)$ , with  $\ell = 2$  and  $p = 3$ , and an HG mode  $E_2(x, y) = H_n(x) H_m(y)$ , with  $n = 1$  and  $m = 2$  [Fig. 2(a) insets]; here  $(r, \varphi)$  and  $(x, y)$  are the polar and Cartesian coordinates, respectively, in the same plane. The structure of the field  $E(x, y) = E_1(x, y) + E_2(x, y)$  (intensity distribution shown in

Fig. 2(a)) may be elucidated by analyzing it in two modal bases, the OAM-LG basis in  $(r, \varphi)$  and the HG basis in  $(x, y)$ . The resulting 2D interferograms  $P(\alpha, \beta)$  in each basis is shown in Figs. 2(b), 2(d). These interferograms are obtained separately by changing the GPOs, potentially implemented using spatial light modulators. Taking the 2D FT of each interferogram we obtain the modal coefficients shown in Figs. 2(c), 2(e). The peak associated with  $E_1$  in the OAM-LG modal analysis is distinct [Fig. 2(c)] while  $E_2$  appears as a superposition of multiple modes. Alternatively, the peak associated with  $E_2$  in the HG modal analysis is distinct [Fig. 1(e)] while  $E_1$  appears as a superposition of multiple modes. Analysis in multiple modal bases, by choosing the appropriate GPOs, thus reveals different and complementary aspects of the field.

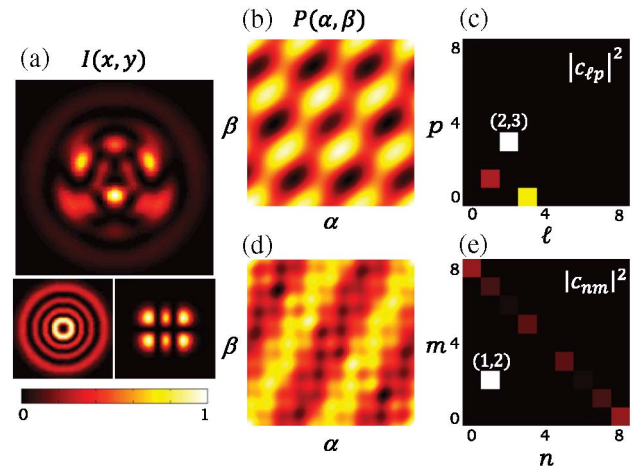


Fig. 2. (Color online) (a) Intensity  $I(x, y) = |E(x, y)|^2$  ( $25.6w_0 \times 25.6w_0$ ;  $w_0$  is the Gaussian beam width parameter). Insets show the two superposed modes. (b)–(c) 2D interferogram and modal analysis in the OAM-LG basis and (d)–(e) in the HG basis. The ranges of  $\alpha$  and  $\beta$  are  $[0, 2\pi]$  and  $[0, 1]$  in (b) and  $[0, 4]$  and  $[0, 4]$  in (d), respectively.

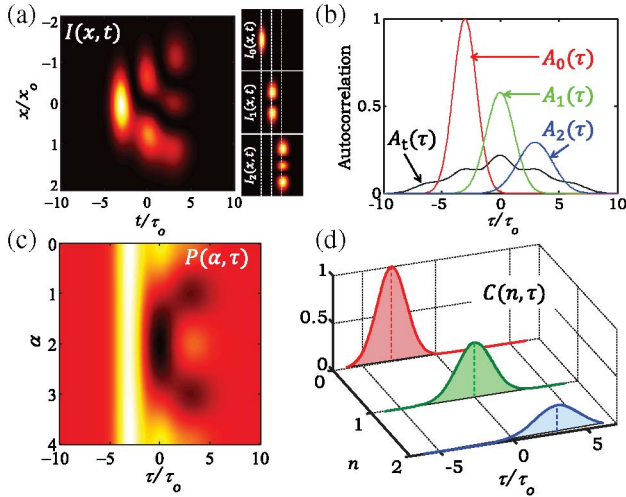


Fig. 3. (Color online) (a) Intensity  $I(x, t) = |E(x, t)|^2$  of three superposed pulsed modes with  $a_1 = a_2 = a_3$ ,  $\frac{t_1}{\tau_0} = -3$ ,  $\frac{t_2}{\tau_0} = 0$ ,  $\frac{t_3}{\tau_0} = 3$ ,  $\frac{T_1}{\tau_0} = 1$ ,  $\frac{T_2}{\tau_0} = 1.2$ ,  $\frac{T_3}{\tau_0} = 1.5$  (see text);  $x_0$  is the Gaussian beam width parameter. The insets are the superposed pulsed modes; the white dotted lines are the pulse centers; (b) spatially integrated temporal autocorrelation of each pulse separately and the superposed pulse; (c) 2D interferogram  $P(\alpha, \tau)$ ; (d) hybrid discrete-continuous modal analysis in the HG basis and time.

Both  $\Lambda_1$  and  $\Lambda_2$  in the previous example correspond to discrete modal bases. A field may alternatively be analyzed into a *hybrid* discrete-continuous 2D modal basis, e.g., *discrete* spatial modes and *continuous* spectral frequency. An example is shown in Fig. 3 for the field  $E(x, t) = \sum_{j=1}^3 a_j H_j(x) f_j(t)$ ;  $f_j(t) = \exp\left(-\frac{(t-t_j)^2}{2\tau_j^2}\right)$  is the pulse envelope after removing a common central frequency. This field is the superposition of three pulses, each having a different HG spatial mode. Such a field may arise when a single-spatial-mode pulse propagates in a multimode waveguide. Modal dispersion may then result in the separation of different pulsed modes. The spatiotemporal intensity distribution of this field is shown in Fig. 3(a), and the spatially integrated temporal autocorrelation is shown in Fig. 3(b) (for each pulse separately and the total field). It is clear that measurements of either DoF while averaging over the other do not reveal the structure of this field. The 2D interferogram  $P(\alpha, \tau)$ , where  $\Lambda_1$  is an fFT of order  $\alpha$  and  $\Lambda_2$  is a delay  $\tau$ , is shown in Fig. 3(c). Taking the FT of  $P(\alpha, \tau)$  with respect to  $\alpha$  alone results in a discrete modal index  $n$  (as in Fig. 2), while  $\tau$  remains continuous,  $C(n, \tau)$ . We thereby

isolate the autocorrelations of the pulses associated with the different spatial modes [see Fig. 3(d)].

Higher-order interferometry may be carried out by utilizing more GPOs, e.g., temporal interference alongside 2D spatial interference to obtain a 3D interferogram. Finally, the observation that a fractional transform is a GPO defined on its eigenfunctions motivates the construction of new transforms. For example, the fractional transform that has Bessel functions (of the first kind) as eigenfunctions enables, in conjunction with the OAM operator, the analysis of the 2D field in a circularly symmetric fiber or waveguide. Finally, we note that the discretization of the parameter  $\alpha$  in a GPO sets the main limitation on the fidelity of the modal analysis.

In conclusion, we have presented a general conception of optical interferometry using an arbitrary degree or degrees of freedom by replacing the optical delay in an interferometer with a generalized phase operator. Placing multiple GPOs in an interferometer enables multidimensional interferometry and modal analysis. Furthermore, when the DOF modal basis is discrete, the GPO corresponds to a fractional transform that has this basis as eigenfunctions.

## References

1. M. Born and E. Wolf, *Principles of Optics* (Cambridge University, 1999).
2. H. M. Ozaktas, Z. Zalevsky, and M. A. Kutay, *The Fractional Fourier Transform* (Wiley, 2001).
3. B. J. Smith, B. Killett, M. G. Raymer, K. Banaszek, and I. A. Walmsley, *Opt. Lett.* **30**, 3365 (2005).
4. L. Allen, S. M. Barnett, and M. J. Padgett, *Optical Angular Momentum* (Institute of Physics, 2003).
5. R. Zambrini and S. M. Barnett, *Phys. Rev. Lett.* **96**, 113901 (2006).
6. J. Leach, M. J. Padgett, S. M. Barnett, S. Franke-Arnold, and J. Courtial, *Phys. Rev. Lett.* **88**, 257901 (2002).
7. H. Wei, X. Xue, J. Leach, M. J. Padgett, S. M. Barnett, S. Franke-Arnold, E. Yaoc, and J. Courtial, *Opt. Commun.* **223**, 117 (2003).
8. V. Namias, *IMA J. Appl. Math.* **26**, 187 (1980).
9. T. Alieva and M. J. Bastiaans, *Opt. Lett.* **24**, 1206 (1999).
10. A. F. Abouraddy, T. M. Yarnall, and B. E. A. Saleh, *Opt. Lett.* **36**, 4683 (2011).
11. X. Xue, H. Wei, and A. G. Kirk, *Opt. Lett.* **26**, 1746 (2001).
12. H. Sasada and M. Okamoto, *Phys. Rev. A* **68**, 012323 (2003).
13. A. F. Abouraddy, T. Yarnall, B. E. A. Saleh, and M. C. Teich, *Phys. Rev. A* **75**, 052114 (2007).
14. T. Yarnall, A. F. Abouraddy, B. E. A. Saleh, and M. C. Teich, *Phys. Rev. Lett.* **99**, 170408 (2007).
15. T. Yarnall, A. F. Abouraddy, B. E. A. Saleh, and M. C. Teich, *Phys. Rev. Lett.* **99**, 250502 (2007).